© Indian Academy of Sciences

CrossMark

Computational model on pulsatile flow of blood through a tapered arterial stenosis with radially variable viscosity and magnetic field

S PRIYADHARSHINI* and R PONALAGUSAMY

Department of Mathematics, National Institute of Technology, Tiruchirappalli 620015, India
e-mail: priya.nit13@gmail.com; rpalagu@nitt.edu

Abstract.   An unsteady two-fluid model of blood flow through a tapered arterial stenosis with variable viscosity in the presence of variable magnetic field has been analysed in the present paper. In this article, blood in the core region is assumed to obey the law of Jeffrey fluid and plasma in the peripheral layer is assumed to be Newtonian. The values for velocity, wall shear stress, flow rate and flow resistance are numerically computed by employing finite-difference method in solving the governing equations. A comparison study between the velocity profiles obtained by the present study and the experimental data represented graphically shows that that the rheology of blood obeys the law of Jeffrey fluid rather than that of Newtonian fluid. The effects of parameters such as taper angle, radially variable viscosity, hematocrit, Jeffrey parameter, magnetic field and plasma layer thickness on physiologically important parameters such as wall shear stress distribution and flow resistance have been investigated. The results in the case of radially variable magnetic field and constant magnetic field are compared to observe the effect of magnetic field in driving the blood flow. It is observed that increase in hematocrit increases the wall shear stress. The values of wall shear stress and flow resistance are obtained at various time instances and compared. It is pertinent to note that the magnitudes of flow resistance are higher in the case of converging tapered than non-tapered and diverging tapered artery.

Keywords.   Jeffrey fluid; radially variable viscosity; hematocrit; radially variable magnetic field; tapered arterial stenosis.

1. Introduction

The blood flow in a stenosed artery and the effect of physical parameters on blood flow was analysed and studied in references [1–4]. Several investigators [5–9] discussed experimental and theoretical studies on blood flow, which are useful in the diagnosis and treatment of cardiovascular diseases. The presence of taper and its implications on physiologically significant parameters have been studied in [10, 11]. Many investigators [12–16] analysed the blood flow in a stenosed artery by assuming blood to be a Newtonian fluid. At low shear stress this is not applicable. Blood is generally assumed to be non-Newtonian due to the presence of formed elements. Haemoglobin is an iron-based protein inside red blood cells [4]. Several investigators [17–24] analysed the effects of magnetic field on blood flow through a stenosed artery. The practical applications of magnetic field in medicine has been investigated by Motta *et al* [25] and Midya *et al* [26]. Nadeem and Ijaz [27] analysed the effects of tapering on blood flow through stenosed artery.

Bugliarello and Sevilla [28] and Cokelet [29] experimentally showed that there exists a cell-free plasma layer in addition to a core region consisting of erythrocytes. Ponalagusamy [30] analysed the blood flow through stenosed arteries with axially variable peripheral layer thickness and variable slip at the wall, considering the fluids in both core and plasma regions as Newtonian. The effects of peripheral plasma layer thickness and yield stress on wall shear stress (WSS) and resistive impedance have been studied by Chaturani and Ponnalagarsamy [31]. Ponalagusamy and Tamil Selvi [32] developed a two-fluid model for blood where fluid in the core region is assumed to be Cassonian and the fluid in the peripheral region to be Newtonian taking slip velocity into account. Sankar and Lee [33] analysed the pulsatile flow of blood through stenosed arteries by assuming blood in the core region to be Cassonian fluid and plasma fluid to be Newtonian. Srivastava [34] investigated the two-phase model of blood flow through stenosed tubes in the presence of a peripheral layer. The problem of non-Newtonian and nonlinear blood flow through a stenosed artery has been analysed and solved by Chaturani and Ponnalagarsamy [35], where the non-Newtonian rheology of the flowing blood is characterized by a Herschel–Bulkley model. Ikbal *et al* [36] investigated

---

*For correspondence

mathematical model on non-Newtonian flow of blood through a stenosed artery in the presence of a transverse magnetic field by treating blood as a power-law fluid. The unsteady nature of blood flow has been further studied by Mustapha *et al* [37] and Eldesoky *et al* [38].

Jeffrey fluid belongs to the class of non-Newtonian fluid. The Jeffrey fluid as a generalization of Newtonian fluid and hence Newtonian fluid can be deduced from the Jeffrey fluid model as a special case. Many investigators have studied the flow of Jeffrey fluid in the presence of several factors. Akbar *et al* [39] have investigated a non-Newtonian fluid model for blood flow through a tapered artery with a stenosis by assuming blood as a Jeffrey fluid taking heat and mass transfer into account. Nallapu and Radhakrishnamacharya [40] developed a mathematical model of blood flow as a two-fluid model where the fluid in the core region is assumed to be a Jeffrey fluid and plasma in peripheral region to be a Newtonian fluid. Jyothi *et al* [41] analysed the flow of blood in a catherized tapered artery with nanoparticles considering blood as a Jeffrey fluid. The flow of Jeffrey fluid has been further discussed in references [42–45]. A non-Newtonian fluid model for blood flow through a tapered artery with a stenosis and variable viscosity by modelling blood as Jeffrey fluid has been developed by Ellahi *et al* [45]. It is of interest to mention that the combined effects of physiologically important parameters such as radially variable core viscosity and magnetic field have not been investigated in the aforementioned mathematical models.

It is argued that the non-homogeneity of blood should be accounted for while investigating the flow of blood in order to have a realistic model [46–48]. These facts imply that the viscosity of blood is a function of hematocrit in such a way that it varies radially more near the tube axis and decreases when one moves towards the arterial wall and becomes a constant in the peripheral plasma layer. Further, fluid dynamics of biological fluids under the influence of magnetic field emerges as a new trend to investigate their flow behaviour in the presence of a magnetic field. In view of these, a modest effort has been made to study the unsteady flow of blood as two-layered blood, where blood in the core region is assumed to be a Jeffrey fluid and plasma in peripheral layer to be Newtonian taking into account variable core viscosity and variable magnetic field.

2. Formulation of the problem

Let us consider an axially symmetric, pulsatile, laminar and fully developed flow of blood in a tapered artery with stenosis and radially variable transverse magnetic field. In the present study, the flow of blood is represented by a two-fluid model where the blood in the core region is assumed to be a Jeffrey fluid and the plasma in the peripheral region

to be a Newtonian fluid. We consider a cylindrical coordinate system $(\bar{r}, \bar{\theta}, \bar{z})$, whose origin is located on the axis of tapered arterial stenosis (figures 1 and 2).

The consistency function $\bar{\mu}(\bar{r})$ may be written as follows:

$$\bar{\mu}(\bar{r}) = \begin{cases} \bar{\mu}_c(\bar{r}), 0 \leq \bar{r} \leq \bar{R}_1(\bar{z}) \\ \bar{\mu}_p, \bar{R}_1(\bar{z}) \leq \bar{r} \leq \bar{R}(\bar{z}) \end{cases} \tag{1}$$

where $\bar{\mu}_c(\bar{r})$ and $\bar{\mu}_p$ are the viscosities of the central core fluid and the plasma, respectively; $\bar{R}_1(\bar{z})$ and $\bar{R}(\bar{z})$ are the radii of the central core region and the artery in the stenotic region. The momentum equations governing the unsteady incompressible Jeffrey fluid in the core region are [42]

$$\frac{\partial \bar{v}_c}{\partial \bar{r}} + \frac{\bar{v}_c}{\bar{r}} + \frac{\partial u_c}{\partial \bar{z}} = 0, \tag{2}$$

$$\bar{\rho}_c \left(\frac{\partial}{\partial \bar{t}} + \bar{v}_c \frac{\partial}{\partial \bar{r}} + \bar{u}_c \frac{\partial}{\partial \bar{z}} \right) \bar{u}_c = -\frac{\partial \bar{p}}{\partial \bar{z}} + \frac{1}{\bar{r}} \frac{\partial}{\partial \bar{r}} (\bar{r} \bar{S}_{rz}) + \frac{\partial}{\partial \bar{z}} (\bar{S}_{zz})$$
$$- \bar{\sigma} \bar{B}_0^2(\bar{r}) \bar{u}_c, \tag{3}$$

$$\bar{\rho}_c \left(\frac{\partial}{\partial \bar{t}} + \bar{v}_c \frac{\partial}{\partial \bar{r}} + \bar{u}_c \frac{\partial}{\partial \bar{z}} \right) \bar{v}_c = -\frac{\partial \bar{p}}{\partial \bar{r}} + \frac{1}{\bar{r}} \frac{\partial}{\partial \bar{r}} (\bar{r} \bar{S}_{rr}) + \frac{\partial}{\partial \bar{z}} (\bar{S}_{rz})$$
$$- \frac{\bar{S}_{\theta\theta}}{\bar{r}}. \tag{4}$$

The extra tensor $\bar{S}$ for Jeffrey fluid is defined as follows:

$$\bar{S} = \frac{\bar{\mu}_c(\bar{r})}{(1 + \lambda_1)} (\dot{\bar{\gamma}} + \bar{\lambda}_2 \ddot{\bar{\gamma}}) \tag{5}$$

where $\dot{\bar{\gamma}}$ is the shear rate, $\ddot{\bar{\gamma}}$ is the rate of shear rate, $\bar{\mu}_c(\bar{r})$ is the viscosity of core fluid and is given by $\bar{\mu}_c(\bar{r}) = \bar{\mu}_p[1 + \beta \bar{h}(\bar{r})]$, $\bar{h}(\bar{r}) = h_m[R_1^{m_2} - r^{m_2}]$, λ_1 is the ratio of relaxation to retardation times, $\bar{\lambda}_2$ is the retardation time, $\bar{p}$ is the pressure, $\bar{\rho}_c$ is the density of the core fluid, $\bar{\sigma}$ is the electrical conductivity of the fluid and $\bar{B}_0^2(\bar{r})$ is the variable magnetic field [39]; $\bar{u}_c$ and $\bar{v}_c$ are the velocity components in the core region along the z and r directions, respectively.

The momentum equations governing the unsteady Newtonian fluid in the peripheral plasma region are

$$\frac{\partial \bar{v}_p}{\partial \bar{r}} + \frac{\bar{v}_p}{\bar{r}} + \frac{\partial \bar{u}_p}{\partial \bar{z}} = 0 \tag{6}$$

$$\bar{\rho}_p \left(\frac{\partial}{\partial \bar{t}} + \bar{v}_p \frac{\partial}{\partial \bar{r}} + \bar{u}_p \frac{\partial}{\partial \bar{z}} \right) \bar{u}_p = -\frac{\partial \bar{p}}{\partial z} + \bar{\mu}_p$$
$$\times \left[\frac{1}{\bar{r}} \frac{\partial}{\partial \bar{r}} \left(\bar{r} \frac{\partial \bar{u}_p}{\partial \bar{r}} \right) + \frac{\partial^2 \bar{u}_p}{\partial \bar{z}^2} \right]$$
$$- \bar{\sigma} \bar{B}_0^2(\bar{r}) \bar{u}_p \tag{7}$$

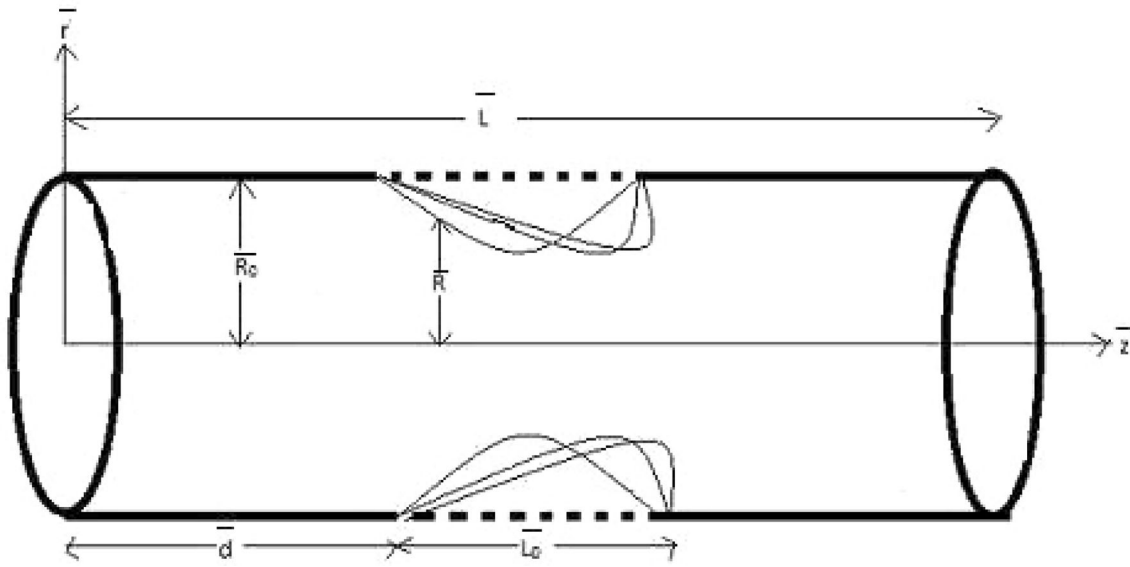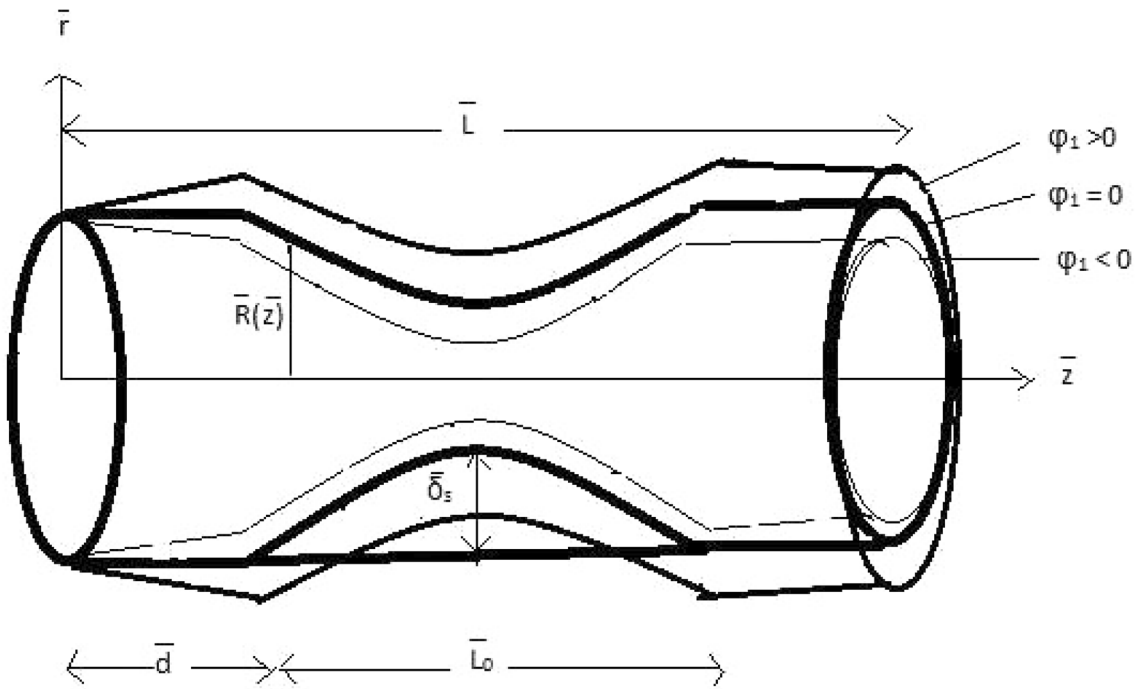**Figure 1.** Geometry of an axially non-symmetrical stenosed artery.

Figure 2. Geometry of the stenosed artery for different taper angles.

$$\bar{\rho_p}\left(\frac{\partial}{\partial \bar{t}}+\bar{v_p}\frac{\partial}{\partial \bar{r}}+\bar{u_p}\frac{\partial}{\partial \bar{z}}\right)\bar{v_p}=-\frac{\partial \bar{p}}{\partial \bar{r}}+\bar{\mu_p}$$

$$\times\left[\frac{1}{\bar{r}}\frac{\partial}{\partial \bar{r}}\left(\bar{r}\frac{\partial \bar{v_p}}{\partial \bar{r}}\right)+\frac{\partial^2 \bar{v_p}}{\partial \bar{z}^2}-\frac{\bar{v_p}}{\bar{r}^2}\right]$$

$$(8)$$

where $\bar{\rho_p}$ is the density of plasma fluid and $\bar{\mu_p}$ is the viscosity of fluid in plasma region; $\bar{u_p}$ and $\bar{v_p}$ are the velocity components of plasma in $\bar{z}$ and $\bar{r}$ directions respectively.

The following non-dimensional variables are introduced:

$$r = \frac{\bar{r}}{\bar{R}_0}, z = \frac{\bar{z}}{\bar{L}_0}, t = \bar{\omega}\bar{t}, u_c = \frac{\bar{u}_c}{\bar{u}_0}, u_p = \frac{\bar{u}_p}{\bar{u}_0}, R_1 = \frac{\bar{R}_1}{\bar{R}_0},$$

$$M^2(r) = \frac{\bar{B}_0^2(\bar{r})\bar{\sigma}\bar{R}_0^2}{\bar{\mu}_p},$$

$$p = \frac{\bar{p}\bar{R}_0^2}{\bar{u}_0\bar{\mu}_p\bar{L}_0}, \rho = \frac{\bar{\rho}_p}{\bar{\rho}_c}, \alpha^2 = \frac{\bar{\rho}_p\bar{\omega}\bar{R}_0^2}{\bar{\mu}_p}, Re = \frac{\bar{\rho}_p\bar{u}_0\bar{R}_0}{\bar{\mu}_p}.$$

$$\tag{9}$$

From literature [49, 50], the values of the average velocity ($\bar{u}_0$) of flow in a uniform artery and its radius ($\bar{R}_0$) are, respectively, taken as 1 cm/s and 0.1 cm.

The appropriate equations in non-dimensional form governing the pulsatile flow of Jeffrey fluid in the case of a slightly tapered artery with mild stenosis (taper angle $< 3^o$ and $\frac{\bar{\delta}_s}{\bar{R}_0} << 1$) are obtained as follows (see Appendix A).

In the core region $(0 \leq r \leq R_1(r))$

$$\frac{\alpha^2}{\rho_0}\frac{\partial u_c}{\partial t} = -\frac{\partial p}{\partial z} + \frac{1}{1 + \lambda_1}\left[\frac{1}{r}\frac{\partial}{\partial r}\right]\left\{1 + \beta h_m\left(R_1^{m_2} - r^{m_2}\right)\right\}$$

$$\frac{\partial u_c}{\partial r} - M^2(r)u_c. \tag{10}$$

In the peripheral plasma region $(R_1(r) \leq r \leq R)$

$$\alpha^2\frac{\partial u_p}{\partial t} = -\frac{\partial p}{\partial z} + \frac{\partial^2 u_p}{\partial r^2} + \frac{1}{r}\frac{\partial u_p}{\partial r} - M^2(r)u_p \tag{11}$$

where $M(r) = Me^{\alpha_1(R-r)}$ [4].

The main motive mechanism for blood flow is the prevailing pressure gradient. The pressure gradient is given by $-\frac{\partial p}{\partial z}(z, t) = A_0 + A_1\cos(t)$.

The corresponding boundary conditions are

  (i) $\frac{\partial u_c}{\partial r} = 0$ at $r = 0$,
  (ii) $u_c = u_p$ at $r = R_1$,
  (iii) $(\tau)_p = (\tau)_c$ at $r = R_1$ and
  (iv) $u_p = 0$ at $r = R$.

The non-dimensional form of flow geometry is given by

$$R(z) = \begin{cases} (1 - \psi z)[1 - B\{(z - d) - (z - d)^{n_1}\}], \\ \qquad\qquad\qquad\qquad\qquad\qquad d \leq z \leq d + 1 \\ 1 - \psi z, \text{otherwise} \end{cases} \tag{12}$$

where $B = \frac{\delta_s n_1^{\frac{n_1}{n_1-1}}}{n_1 - 1}$, $\psi = \tan\phi$ and ϕ is the taper angle. For converging tapering, ϕ becomes greater than 0, $\phi < 0$ indicates diverging tapering and $\phi = 0$ for the case of non-tapered artery (arterial stenosis).

3. Solution of the problem

The implicit difference scheme for Eq. (10) is as follows [51]:

$$u_c = \frac{(u_c)_{i,j}^{k+1} + (u_c)_{i,j}^k}{2},$$

$$\frac{\partial u_c}{\partial t} = \frac{(u_c)_{i,j}^{k+1} - (u_c)_{i,j}^k}{\Delta t},$$

$$\frac{\partial u_c}{\partial r} = \frac{(u_c)_{i,j+1}^{k+1} - (u_c)_{i,j-1}^{k+1} + (u_c)_{i,j+1}^k - (u_c)_{i,j-1}^k}{4\Delta r},$$

$$\frac{\partial^2 u_c}{\partial r^2} = \frac{(u_c)_{i,j+1}^{k+1} - 2(u_c)_{i,j}^{k+1} + (u_c)_{i,j-1}^{k+1} + (u_c)_{i,j+1}^k - 2(u_c)_{i,j}^k + (u_c)_{i,j-1}^k}{2(\Delta r)^2}.$$

$$\tag{13}$$

Using these finite-difference approximations (13), Eq. (10) becomes

$$\left[\frac{X(r_j)}{2(\Delta r)^2} + \frac{S(r_j)}{4\Delta r}\right](u_c)_{i,j+1}^{k+1} - \left[\frac{X(r_j)}{(\Delta r)^2} + \frac{\alpha^2}{\Delta t} + \frac{M^2(r_j)}{2}\right](u_c)_{i,j}^{k+1}$$

$$+ \left[\frac{X(r_j)}{2(\Delta r)^2} - \frac{S(r_j)}{4\Delta r}\right](u_c)_{i,j-1}^{k+1}$$

$$= -(A_0 + A_1\cos(t^k)) - \left[\frac{X(r_j)}{2(\Delta r)^2} + \frac{S(r_j)}{4\Delta r}\right](u_c)_{i,j+1}^k$$

$$+ \left[\frac{X(r_j)}{(\Delta r)^2} + \frac{\alpha^2}{\Delta t} + \frac{M^2(r_j)}{2}\right](u_c)_{i,j}^k$$

$$- \left[\frac{X(r_j)}{2(\Delta r)^2} - \frac{S(r_j)}{4\Delta r}\right](u_c)_{i,j-1}^k \tag{14}$$

where

$$X(r_j) = r_j\left[1 + \beta h_m\left(R_1^{m_2} - r_j^{m_2}\right)\right],$$

$$S(r_j) = \frac{1}{(1 + \lambda_1)r_j}\left[1 + \beta h_m\left(R_1^{m_2} - (m_2 + 1)r_j^{m_2}\right)\right].$$

Adopting the following implicit scheme:

$$u_p = \frac{(u_p)_{i,j}^{k+1} + (u_p)_{i,j}^k}{2},$$

$$\frac{\partial u_p}{\partial t} = \frac{(u_p)_{i,j}^{k+1} - (u_p)_{i,j}^k}{\Delta t},$$

$$\frac{\partial u_p}{\partial r} = \frac{(u_p)_{i,j+1}^{k+1} - (u_p)_{i,j-1}^{k+1} + (u_p)_{i,j+1}^k - (u_p)_{i,j-1}^k}{4\Delta r},$$

$$\frac{\partial^2 u_p}{\partial r^2} = \frac{(u_p)_{i,j+1}^{k+1} - 2(u_p)_{i,j}^{k+1} + (u_p)_{i,j-1}^{k+1} + (u_p)_{i,j+1}^k - 2(u_p)_{i,j}^k + (u_p)_{i,j-1}^k}{2(\Delta r)^2},$$

$$\tag{15}$$

Eq. (11) becomes

$$
\begin{aligned}
&\left[\frac{r_j}{2(\Delta r)^2} + \frac{1}{4\Delta r}\right](u_p)_{i,j+1}^{k+1} - \left[\frac{r_j}{(\Delta r)^2} + \frac{r_j\alpha^2}{\Delta t} + \frac{M^2(r_j)}{2}\right](u_p)_{i,j}^{k+1} \\
&+ \left[\frac{r_j}{2(\Delta r)^2} - \frac{1}{4\Delta r}\right](u_p)_{i,j-1}^{k+1} = -r_j(A_0 + A_1\cos(t^k)) \\
&- \left[\frac{r_j}{2(\Delta r)^2} + \frac{1}{4\Delta r}\right](u_p)_{i,j+1}^{k} + \left[\frac{r_j}{(\Delta r)^2} + \frac{r_j\alpha^2}{\Delta t} + \frac{M^2(r_j)}{2}\right](u_p)_{i,j}^{k} \\
&- \left[\frac{r_j}{2(\Delta r)^2} - \frac{1}{4\Delta r}\right](u_p)_{i,j-1}^{k}
\end{aligned}
$$

$$(16)$$

where $M(r_j) = Me^{\alpha_1(R-r_j)}$ [4]. Equations (14) and (16) are solved by the Thomas algorithm to obtain velocities in the core region and plasma region, respectively. In order to solve Eqs. (14) and (16) we need initial velocities for u_c and u_p.

In the case of a two-fluid flow with radially variable magnetic field, the initial velocities for u_c and u_p can be numerically obtained from

$$
0 = (A_0 + A_1) + \frac{1}{1+\lambda_1}\left[\frac{\partial^2 u_c}{\partial r^2} + \frac{1}{r}\frac{\partial u_c}{\partial r}\right] - M^2(r)u_c, \quad (17)
$$

$$
0 = (A_0 + A_1) + \frac{\partial^2 u_p}{\partial r^2} + \frac{1}{r}\frac{\partial u_p}{\partial r} - M^2(r)u_p. \quad (18)
$$

Using the following finite-difference approximations in Eqs. (17) and (18)

$$
\frac{\partial u_c}{\partial r} = \frac{(u_c)_{i,j+1} - (u_c)_{i,j}}{\Delta r}, \frac{\partial^2 u_c}{\partial r^2} = \frac{(u_c)_{i,j+1} - 2(u_c)_{i,j} + (u_c)_{i,j-1}}{(\Delta r)^2},
$$

$$
\frac{\partial u_p}{\partial r} = \frac{(u_p)_{i,j+1} - (u_p)_{i,j}}{\Delta r}, \frac{\partial^2 u_p}{\partial r^2} = \frac{(u_p)_{i,j+1} - 2(u_p)_{i,j} + (u_p)_{i,j-1}}{(\Delta r)^2},
$$

$$(19)$$

we get the following difference equations:

$$
\begin{aligned}
-(A_0 + A_1)(1+\lambda_1)r_j = &\left[\frac{r_j}{(\Delta r)^2} + \frac{1}{\Delta r}\right](u_c)_{i,j+1} \\
&- \left[\frac{2r_j}{(\Delta r)^2} + \frac{1}{\Delta r} + (1+\lambda_1)r_j\right. \\
&\left. M^2(r_j)\right](u_c)_{i,j} + \frac{r_j}{\Delta r)^2}(u_c)_{i,j-1},
\end{aligned}
$$

$$(20)$$

$$
\begin{aligned}
-(A_0 + A_1)r_j = &\left[\frac{r_j}{(\Delta r)^2} + \frac{1}{\Delta r}\right](u_p)_{i,j+1} \\
&- \left[\frac{2r_j}{(\Delta r)^2} + \frac{1}{\Delta r} + r_j M^2(r_j)\right](u_p)_{i,j} \quad (21) \\
&+ \frac{r_j}{(\Delta r)^2}(u_p)_{i,j-1}.
\end{aligned}
$$

Solving this system of equations, initial values for u_c and u_p can be obtained.

The non-dimensional shear stress in the core region is given by

$$
\mathbf{S}_{rz} = \frac{1 + \beta h_m\left(R_1^{m_2} - r^{m_2}\right)}{1 + \lambda_1}\frac{\partial u_c}{\partial r}. \quad (22)
$$

The non-dimensional form of shear stress in the plasma region is expressed as follows:

$$
\mathbf{S}_{rz} = \frac{\partial u_p}{\partial r}. \quad (23)
$$

The non-dimensional shear stress at the wall is given as follows:

$$
\tau_w = \left(\frac{\partial u_p}{\partial r}\right)_{r=R}. \quad (24)
$$

The flow rate $Q_c(z,t)$ in the core region can be obtained from the relation

$$
Q_c(z,t) = 2\sum_{r=0}^{R_1(z)} r u_c(r,z,t)\Delta r. \quad (25)
$$

The flow rate $Q_p(z,t)$ in the peripheral plasma region is given by the relation

$$
Q_p(z,t) = 2\sum_{r=R_1(z)}^{R(z)} r u_p(r,z,t)\Delta r. \quad (26)
$$

The total flow rate is $Q(z,t) = Q_c(z,t) + Q_p(z,t)$, which implies

$$
\begin{aligned}
Q(z,t) = &2\sum_{r=0}^{R_1(z)} r u_c(r,z,t)\Delta r \\
&+ 2\sum_{r=R_1(z)}^{R(z)} r u_p(r,z,t)\Delta r
\end{aligned} \quad (27)
$$

where $R_1(z) = \gamma R(z), \gamma = 1 - \frac{\delta(z)}{R(z)}$ and $\delta(z)$ is the plasma layer thickness [4].

The flow resistance λ is defined as follows:

$$\lambda = \sum_{0}^{z} \left[\frac{-\frac{\partial p}{\partial z}(z,t)}{Q(z,t)} \right] \Delta z \qquad (28)$$

where z is any point in the section of tapered arterial stenosis. Flow resistance values are obtained by substituting $-\frac{\partial p}{\partial z}(z,t) = A_0 + A_1 \cos t$ and Eq. (27) in Eq. (28).

4. Results and discussion

The governing equations of the system are solved numerically using Crank–Nicholson finite-difference schemes to discretize the spacial derivatives. The flow region has been discretized by taking the step size in the radial direction $\Delta r = 0.001$ and the time step size is taken to be $\Delta t = 0.001$ in order to guarantee the convergence of the numerical solution to the sixth order. Hence, the solution domain (the $r - z$ plane) is divided into 10,00,000 meshes in order to compute the required numerical results, which could be useful to predict the actual flow phenomenon. Also, it is observed that further reduction in Δr and Δt does not bring about any substantial change, which leads to the stability of the numerical techniques. MATLAB programming codes are developed to compute the numerical values for velocity profile, WSS and flow resistance for different values of the parameters involved in the present study.

When blood flows in a uniform artery, the variation of the axial velocity profiles of the one-fluid model for the steady flow of Newtonian fluid and the two-fluid model consisting of Jeffrey fluid in the core region and Newtonian fluid in the peripheral region along with the experimental results of [28] for blood containing 40% RBC has been displayed in figure 3. It is observed that the rheology of blood behaves like that of a Jeffrey fluid than that of a Newtonian fluid. A comparative study of the present numerical results with the corresponding steady-flow solutions obtained by [40] and the steady flow of Newtonian fluid has been shown in figure 3. One of the remarkable results is that the axial velocity obtained from the present study seems to be closer to the experimental result [28] for $\beta = 2, m_2 = 2, h_m = 0.4, \lambda_1 = 0.1$. Based on the results obtained from the present investigation, one may infer that the Jeffrey parameter, variable viscosity and the plasma layer thickness affect the axial flow velocity. Hence it is important to analyse the effect of these parameters in this blood flow model. It is pertinent to point out here that good agreement between the present results and the experimental results [28] has been found, in the sense that the experimental results lie within the range of the presently computed values as displayed in figure 3.

The axial variation of WSS for different values of parameters involved in the present study is depicted in figures 4–7. Figures 4– 7 show that there is an increase in the WSS until it reaches the midpoint of the stenotic region, and decreases in the downstream of the region. The effect
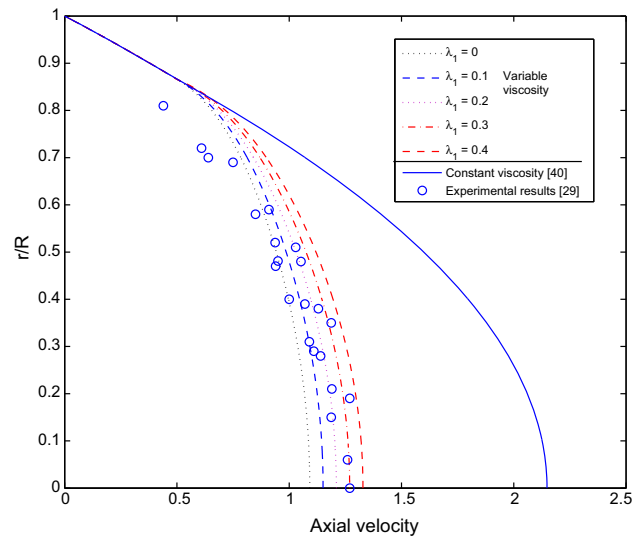

Figure 3. Velocity distribution with radial distance.

of maximum stenotic height (δ_s) can be observed from figure 4. As the stenotic height increases, the WSS increases. Figure 5 shows the variation of WSS with axial distance for different values of radially variable magnetic field. Increase in parameter α_1 causes WSS to increase. The magnitude of WSS is comparatively lower in the case of Jeffrey fluid without magnetic field. Therefore the presence of magnetic field induces higher shear stress at the wall.

Figure 6 is plotted to see the axial variation of WSS in the presence of a constant magnetic field and variable magnetic field for the cases of converging tapered ($\psi = 0.01$), non-tapered ($\psi = 0$) and diverging tapered artery ($\psi = -0.01$). It can be observed from figure 6 that WSS increases in the upstream of the stenotic region, reaches maximum at the midpoint of the throat and decreases in the downstream of the region. WSS is found to be more in converging tapered artery than in non-tapered and diverging tapered artery. The variation of WSS in case of variable magnetic field is comparatively higher than in constant magnetic field. It is pertinent to note that as compared with Jeffrey fluid with variable magnetic fluid, WSS is higher in the case of constant magnetic field. Figure 7 shows the effects of time parameter t together with pulsatile Reynolds number α^2. The results presented in figure 7 reveal that WSS is negatively increased as the pulsatile Reynolds number α^2 increases for a given value of time t.

The important predictions of the present investigation are enumerating the combined effects of different values of Jeffrey parameter (λ_1), the plasma layer thickness (in terms of γ), the magnetic parameter (M), the parameter (α_1) involved in the expression of radially variable magnetic field, the taper angle (ψ), the parameters involved in the expression of core fluid viscosity (β, h_m, m_2) , time t, the pulsatile Reynolds number (α^2) and the axial distance (z) on
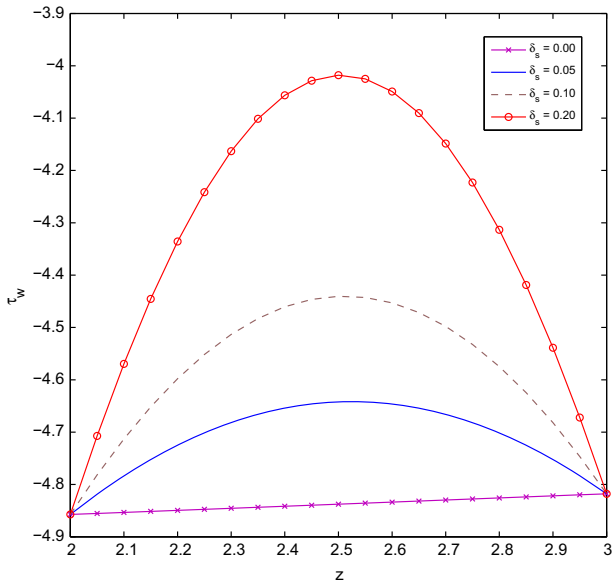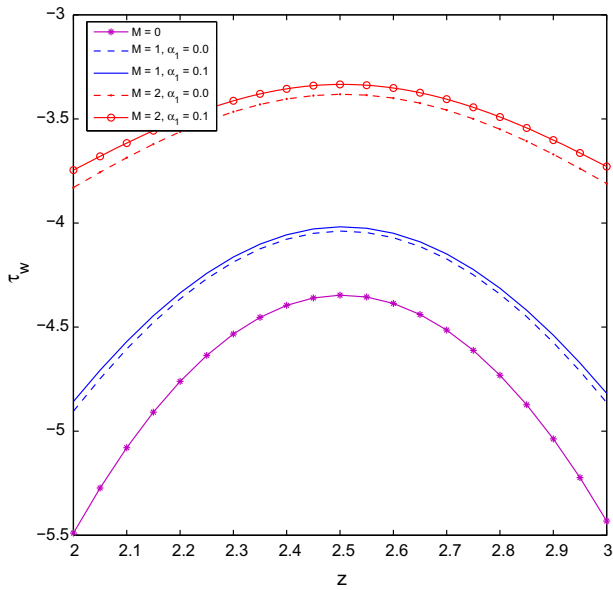
Figure 4. Variation of wall shear stress with axial distance for different values of maximum stenotic height (δ_s) taking $\beta = 2, h_m = 0.4, m_2 = 2, \psi = 0.01, \alpha^2 = 1, \lambda_1 = 0.1, \gamma = 0.8$ and $t = 1$.
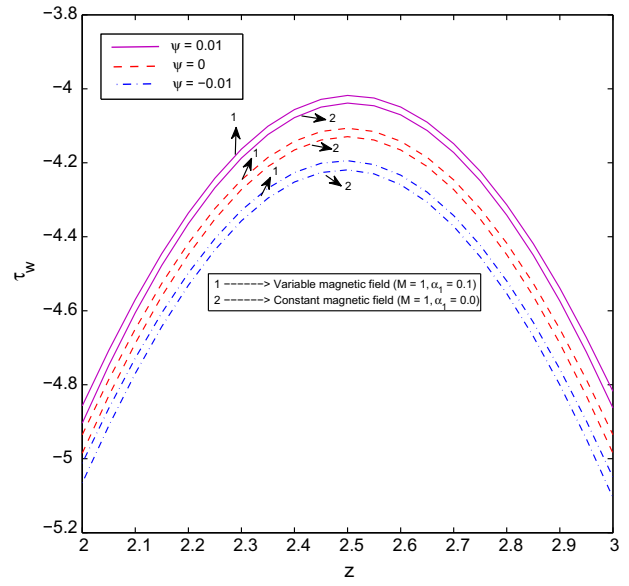
Figure 6. Axial variation of wall shear stress for different values of ψ with respect to constant magnetic field and variable magnetic field taking $\beta = 2, h_m = 0.4, m_2 = 2, \psi = 0.01, \alpha^2 = 1, \lambda_1 = 0.1, \gamma = 0.8$ and $t = 1$.
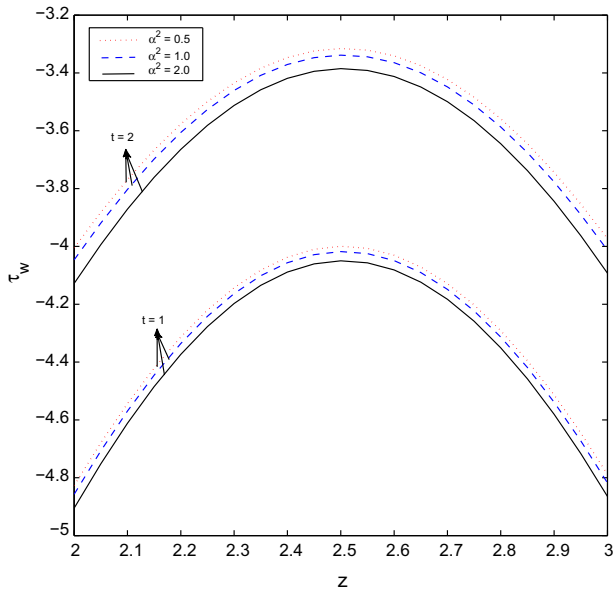

Figure 5. Variation of wall shear stress with axial distance for different values of M and α_1 taking $\beta = 2, h_m = 0.4, m_2 = 2, \psi = 0.01, \alpha^2 = 1, \lambda_1 = 0.1, \gamma = 0.8$ and $t = 1$.

the resistive impedance (figures 8–12). Figure 8 displays the influence of peripheral layer thickness on the resistive impedance when the other parameters are held constant. The increase in the peripheral plasma layer thickness (or a decrease in the parameter γ) leads to a decrease in the resistive impedance. Figure 8 reveals that for a lower value of peripheral plasma layer thickness, the percentage of increase in the axial variation of flow resistance becomes

high but this behaviour becomes less dominant for a higher value of peripheral plasma layer thickness.

Figure 9 depicts the effect of radially variable magnetic field on resistive impedance. It is observed from figure 9 that the blood flow experiences higher resistive impedance for larger values of magnetic field parameter M. It is of interest to mention that the nature of radially varying magnetic field induces higher flow resistance in comparison with that of a constant applied magnetic field. Blood flowing through the tapered arterial stenosis experiences lower flow resistance in the case of Jeffrey fluid without magnetic field than in the presence of magnetic field. Hence, it can be argued that the presence of magnetic field slows down the blood flow, which is further aggravated by increasing the parameter α_1 involved in the expression of radially variable magnetic field. As the value of the parameter α_1 increases, the rate of increase in the flow resistance is less for the lower value of magnetic number M whereas it becomes higher for the higher value of magnetic number M. Figure 10 displays the axial variation of flow resistance with respect to constant and variable magnetic fields in the case of converging tapered, non-tapered and diverging tapered artery. The nature of radially variable magnetic field makes flowing blood to experience more resistive impedance. Converging tapered artery exhibits comparatively high resistive impedance than non-tapered and diverging tapered arteries.
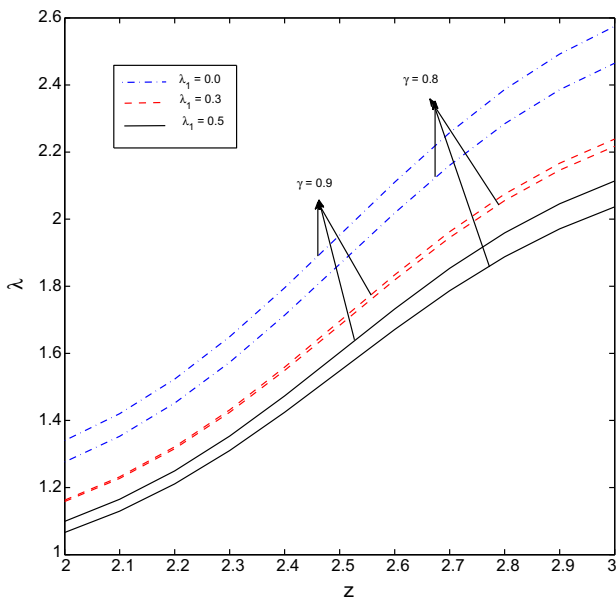
The numerical values of flow resistance for different values of axial distance and the parameters (β, h_m, m_2) involved in the core viscosity have been computed and displayed in figure 11. Hematocrit is the main factor that
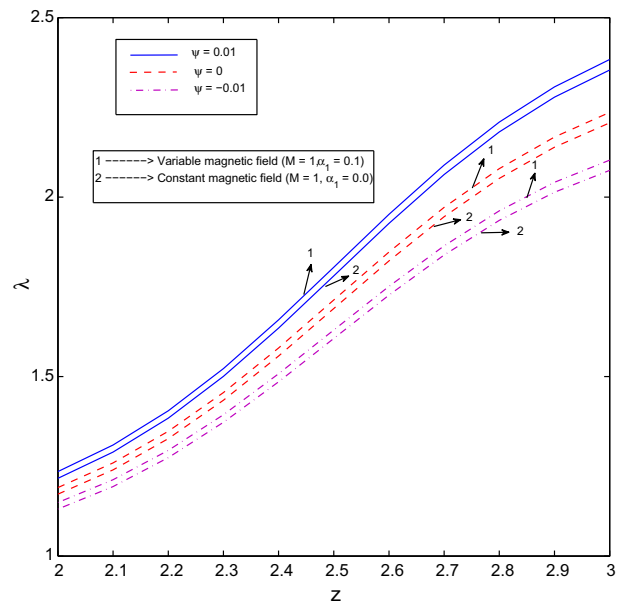
Figure 7. Axial variation of wall shear stress for different values of α^2 and t taking $\beta = 2, h_m = 0.4, m_2 = 2, \psi = 0.01, \lambda_1 = 0.3, \gamma = 0.8, M = 2$ and $\alpha_1 = 0.1$.
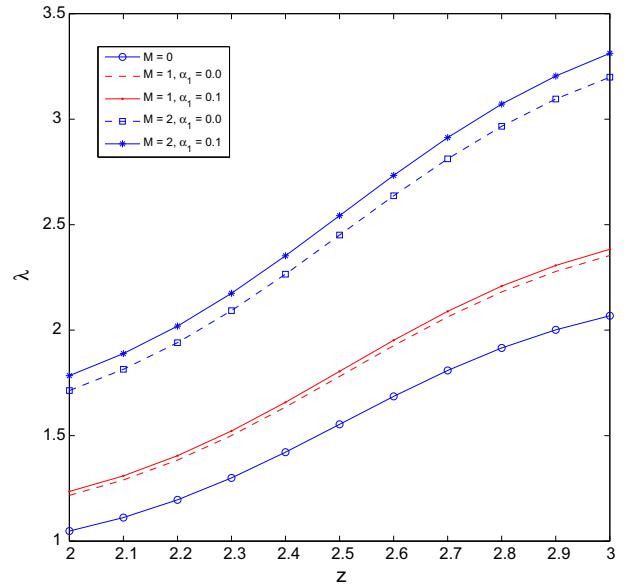
Figure 9. Variation of resistive impedance (λ) with axial distance for different values of M and α_1 taking $\beta = 2, h_m = 0.4, m_2 = 2, \psi = 0.01, \alpha^2 = 1, \lambda_1 = 0.1, \gamma = 0.8$ and $t = 1$.

Figure 8. Axial variation of flow resistance (λ) for different values of λ_1 and γ taking $\beta = 2, h_m = 0.4, m_2 = 2, \psi = 0.01, \alpha^2 = 1, M = 1, \alpha_1 = 0.1$ and $t = 1$.
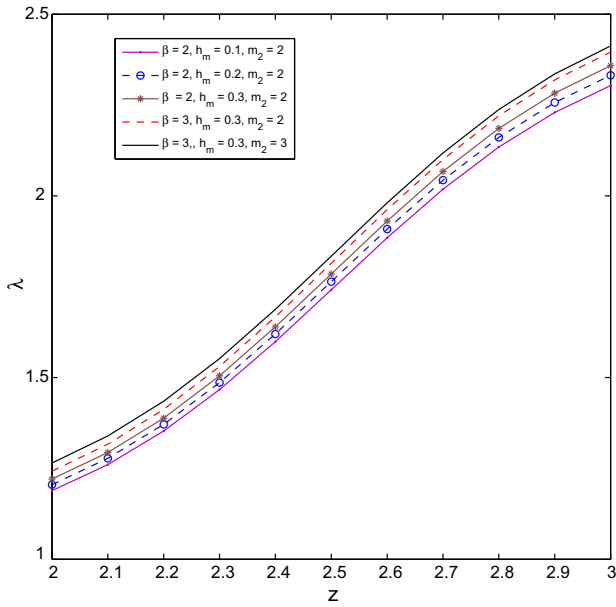

Figure 10. Axial variation of flow resistance (λ) for different values of ψ with respect to constant magnetic field and variable magnetic field taking $\beta = 2, h_m = 0.4, m_2 = 2, \psi = 0.01, \alpha^2 = 1, \lambda_1 = 0.1, \gamma = 0.8$ and $t = 1$.

determines the blood viscosity. The resistance to flow increases as hematocrit level increases. Increase in β leads to increase in flow resistance. The pertinent role of the parameter m_2 involved in the profile of core viscosity has been studied and it is observed that increase in the parameter m_2 leads to decrease in the flow resistance, which

is a new information, for the first time, added to the literature. The significance of unsteady nature of blood flow can be observed from figure 12. As time parameter t increases, the resistance to flow increases. The magnitudes of flow resistances are higher in the case of blood flow in unsteady state than in steady state.

Figure 11. Variation of flow resistance with axial distance for different values of parameters β, h_m, m_2 involved in variable viscosity taking $\psi = 0.01, \alpha^2 = 1, \lambda_1 = 0.1, \gamma = 0.8, M = 1, \alpha_1 = 0.1$ and $t = 1$.
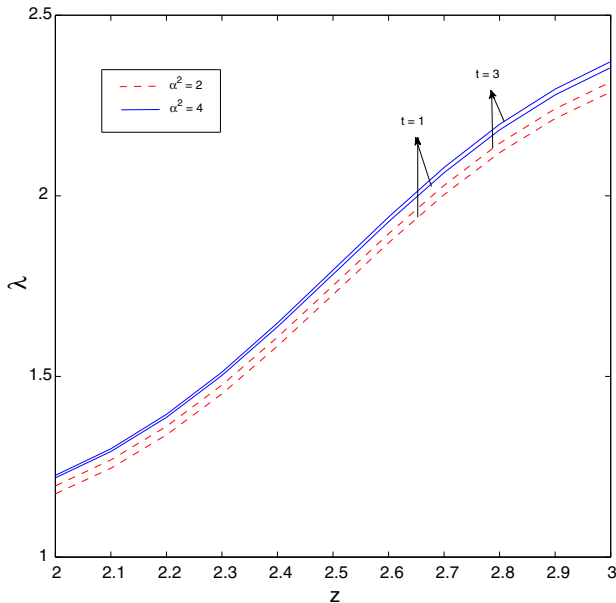
Figure 12. Axial variation of flow resistance for different values of α^2 and t taking $\beta = 2, h_m = 0.4, m_2 = 2, \psi = 0.01, \lambda_1 = 0.1, \gamma = 0.8, M = 1$ and $\alpha_1 = 0.1$.

5. Conclusion

The present mathematical model sheds new light on investigating the combined effects of Jeffrey parameter, peripheral layer thickness, magnetic field parameter, taper angle, hematocrit, the parameters (β, m_2) involved in profile of core

viscosity and time on the physiologically important quantities such as WSS and resistive impedance. Two-fluid models have been considered where the fluid in the core region is assumed to be a Jeffrey fluid and plasma in the peripheral plasma region as a Newtonian fluid with variable viscosity under the influence of variable magnetic field. Furthermore, the parameters involved in the present investigation certainly bear the potential to influence the flow characteristics such as flow velocity, WSS and flow resistance to considerable extent. The flow variables such as velocity, WSS and flow resistance are computed numerically. It is pertinent to point out here that there is a good agreement between the present results and the experimental results [28] and it has been found that that the experimental results lie within the range of the presently computed values of axial velocity as displayed in figure 3.

It is well known that accurately measuring the arterial WSS in the case of pulsatile flow in a tapered stenosed tube is very difficult and 20–50% experimental errors might occur in the estimation of WSS [7]. Furthermore, the inter-correlation between the fluid characteristics and atherosclerotic infection exposes a prevailing association during higher value of WSS, pulsatile nature of WSS, intimal condensing and plaque formation [2, 6, 46]. Hence, a precise prediction of WSS distribution is particularly useful in the thorough understanding of the effects of blood flow on endothelial cells. In view of importance of analysing the variation of WSS with respect to parameters involved in the present work, figures 4–7 have been prepared for the WSS distribution. It is observed that WSS is increased by increasing the values of Jeffrey parameter, magnetic number (Hartmann number), the parameters β, α_1, hematocrit and the nature of converging tapered artery. The increase in the peripheral plasma layer thickness (or a decrease in the parameter γ), the parameter (m_2) and pulsatile Reynolds number (α^2) leads to a decrease in WSS.

The resistive impedance has been thought to be one of the physiologically important flow variables, which is to be investigated along with the effects of other parameters on it due to the fact that it envisages whether the required amount of blood (carrying nutrients and oxygen) supply to vital organs (heart, brain, kidneys, etc.) is ensured or not. The influence of the radially variable magnetic field and constant magnetic field on the flow resistance and WSS has been thoroughly investigated due to their various applications in medical sciences, including transport of drugs using magnetic particles as drug carriers for targeted drug delivery, reducing blood flow at the time of surgery, separating red cells from blood and cancer tumour treatment. The peripheral plasma layer thickness, the rheological behaviour of blood as a Jeffrey fluid, the constant applied magnetic field, the diverging tapered arterial stenosis and the power-law parameter involved in the core fluid viscosity reduce the resistance to flow, which, in turn, leads to normalizing the exiting abnormal blood flow to a greater extent and ultimately preventing sudden death.

It is theoretically observed in the present study that as compared with the case of flow in a non-tapered arterial stenosis, the percentage increase in WSS at the midpoint of stenotic region ($z = 2.5$) due to the presence of convergent tapering in the stenosed artery becomes 12.39% while the percentage decrease in WSS (at $z = 2.5$) due to the presence of divergent tapering in the stenosed artery becomes 10.41%. Further, the percentage increase in the flow resistance (at $z = 3.0$) due to the presence of convergent tapering in the stenosed artery becomes 41.84% while the percentage decrease in the flow resistance (at $z = 3.0$) due to the presence of divergent tapering in the stenosed artery becomes 24.67%. The observed results show that the effect of tapering in blood vessel on flow characteristics (WSS and flow resistance) is significant even for the case of mild tapering ($\psi = 0.05$ or -0.05).

Although the present analysis enlightens the effects of pulsatility, radially variable magnetic field and core fluid viscosity, non-uniform cross-section of artery and non-Newtonian rheology on the flow characteristics, the mathematical model has to be further extended by taking into account several properties of blood. Apart from the pulsatile nature of the blood flow, blood is a concentrated mixture of viscoelastic particles. Blood flow in the arteries shows many other fluid dynamic complexities such as curvature, viscoelastic nature, tapering, narrowing and branching, and hence velocity, flow rate, WSS and resistive impedance will be affected by these phenomena [52]. Further, the motion and nature of the arterial wall are to be considered. Hence, an active research has to be performed in these directions to develop a realistic model that overcomes the limitations of this study. In view of this, a modest effort will be made to investigate the problem of blood flow by incorporating the factors mentioned earlier (two or three factors at a time, impossible to consider all the factors simultaneously) and the numerical findings will be published in the future papers.

Acknowledgements

List of symbols

Dimensional

$\bar{z}$	axial distance
$\bar{r}$	radial distance
$\bar{t}$	time
$\bar{R}_1(\bar{z})$	radius of the central core region
$\bar{R}(\bar{z})$	radius of the artery in the stenotic region
$\bar{u}_c$	axial velocity of the core fluid
$\bar{v}_c$	radial velocity of the core fluid
$\bar{u}_p$	axial velocity of plasma
$\bar{v}_p$	radial velocity of plasma
$\bar{p}$	pressure
$\bar{B}_0^2(\bar{r})$	variable magnetic field
$\bar{\mu}(\bar{r})$	consistency function
$\bar{\mu}_c(\bar{r})$	variable viscosity of the central core fluid
$\bar{\mu}_p$	viscosity of the plasma
$\bar{\rho}_c$	density of the central core fluid
$\bar{\rho}_p$	density of plasma
$\bar{\sigma}$	electrical conductivity of the fluid
$\bar{\lambda}_2$	retardation time

Non-dimensional

δ_s	maximum stenotic height
d	location of the stenosis
n_1	shape of stenosis
ψ	taper angle
λ_1	ratio of relaxation to retardation times
A_0	amplitude of steady pressure gradient
A_1	amplitude of pulsatile pressure gradient
β	constant in variable core viscosity
h_m	hematocrit
Q_c	flow rate in the core region
Q_p	flow rate in the peripheral plasma region
Q	total flow rate
M	magnitude of magnetic field strength
α_1	constant in variable magnetic field
S_{rz}	shear stress
τ_w	wall shear stress
δ	plasma layer thickness
λ	flow resistance

Appendix A

The continuity and momentum equations governing the pulsatile flow of Jeffrey fluid in the presence of magnetic field are given by (Eqs. (2)–(4)) in section 2)

$$\frac{\partial \bar{v}_c}{\partial \bar{r}} + \frac{\bar{v}_c}{r} + \frac{\partial \bar{u}_c}{\partial \bar{z}} = 0 \qquad (A-1)$$

$$\bar{\rho}_c\left(\frac{\partial \bar{u}_c}{\partial \bar{t}} + \bar{v}_c\frac{\partial \bar{u}_c}{\partial \bar{r}} + \bar{u}_c\frac{\partial \bar{u}_c}{\partial \bar{z}}\right) = -\frac{\partial p}{\partial z} + \frac{1}{r}\frac{\partial}{\partial \bar{r}}(\bar{r}\bar{S}_{rz})$$
$$+ \frac{\partial}{\partial \bar{z}}(\bar{S}_{zz}) - \bar{\sigma}\bar{B}_0^2(\bar{r})\bar{u}_c$$
$$(A-2)$$

$$\bar{\rho}_c\left(\frac{\partial \bar{v}_c}{\partial \bar{t}} + \bar{v}_c\frac{\partial \bar{v}_c}{\partial \bar{r}} + \bar{u}_c\frac{\partial \bar{v}_c}{\partial \bar{z}}\right) = -\frac{\partial p}{\partial r} + \frac{1}{r}\frac{\partial}{\partial \bar{r}}(\bar{r}\bar{S}_{rr}) + \frac{\partial}{\partial \bar{z}}(\bar{S}_{rz})$$
$$- \frac{\bar{S}_{\theta\theta}}{\bar{r}}$$
$$(A-3)$$

where the stress components are expressed as follows:

$$\bar{S}_{rr} = \frac{2\bar{\mu}_c(\bar{r})}{1+\lambda_1}\left[1 + \bar{\lambda}_2\left(\bar{v}_c\frac{\partial}{\partial\bar{r}} + \bar{u}_c\frac{\partial}{\partial\bar{z}}\right)\right]\frac{\partial\bar{v}_c}{\partial\bar{r}}, \qquad \text{(A-4)}$$

$$\bar{S}_{rz} = \frac{\bar{\mu}_c(\bar{r})}{1+\lambda_1}\left[1 + \bar{\lambda}_2\left(\bar{v}_c\frac{\partial}{\partial\bar{r}} + \bar{u}_c\frac{\partial}{\partial\bar{z}}\right)\right]\left(\frac{\partial\bar{v}_c}{\partial\bar{z}} + \frac{\partial\bar{u}_c}{\partial\bar{r}}\right), \qquad \text{(A-5)}$$

$$\bar{S}_{zz} = \frac{2\bar{\mu}_c(\bar{r})}{1+\lambda_1}\left[1 + \bar{\lambda}_2\left(\bar{v}_c\frac{\partial}{\partial\bar{r}} + \bar{u}_c\frac{\partial}{\partial\bar{z}}\right)\right]\frac{\partial\bar{u}_c}{\partial\bar{z}}, \qquad \text{(A-6)}$$

$$\bar{S}_{\theta\theta} = \frac{2\bar{\mu}_c(\bar{r})}{1+\lambda_1}\left[1 + \bar{\lambda}_2\left(\bar{v}_c\frac{\partial}{\partial\bar{r}} + \bar{u}_c\frac{\partial}{\partial\bar{z}}\right)\right]\frac{\bar{u}_c}{\bar{r}}. \qquad \text{(A-7)}$$

Using non-dimensionalization as in Eq. (9), the governing equations in dimensionless form are given as follows:

$$\delta_s\left(\frac{\partial v_c}{\partial r} + \frac{v_c}{r}\right) + \frac{\partial u_c}{\partial z} = 0 \qquad \text{(A-8)}$$

$$\frac{\alpha^2}{\rho_0}\frac{\partial u_c}{\partial t} + \frac{Re\bar{\delta}_s}{\bar{L}_0}v_c\frac{\partial u_c}{\partial r} + Re\epsilon u_c\frac{\partial u_c}{\partial z} = -\frac{\partial p}{\partial z} + \frac{1}{r}\frac{\partial}{\partial r}(rS_{rz})$$
$$+ \epsilon^2\frac{\partial}{\partial z}(S_{zz}) - M^2 u_c \qquad \text{(A-9)}$$

$$\frac{\alpha^2}{\rho_0}\delta_s\epsilon^2\frac{\partial v_c}{\partial t} + \frac{Re}{\rho_0}\delta_s^2\epsilon^3 v_c\frac{\partial v_c}{\partial r} + Re\delta_s\epsilon^3 u_c\frac{\partial v_c}{\partial z} = -\frac{\partial p}{\partial r}$$
$$+ \epsilon^2\frac{1}{r}\frac{\partial}{\partial r}(rS_{rr}) + \epsilon^2\frac{\partial}{\partial z}(S_{rz}) - \epsilon^2\frac{S_{\theta\theta}}{r} \qquad \text{(A-10)}$$

where

$$S_{rr} = \frac{2\delta_s}{1+\lambda_1}f_1(r)\left\{1 + \lambda_2\delta_s\left(v_c\frac{\partial}{\partial r} + \frac{u_c}{\delta_s}\frac{\partial}{\partial z}\right)\right\}\left(\frac{\partial v_c}{\partial r}\right) \qquad \text{(A-11)}$$

$$S_{rz} = \frac{f_1(r)}{1+\lambda_1}\left\{1 + \lambda_2\delta_s\left(v_c\frac{\partial}{\partial r} + \frac{u_c}{\delta_s}\frac{\partial}{\partial z}\right)\right\}\left(\delta_s\epsilon^2\frac{\partial v_c}{\partial z} + \frac{\partial u_c}{\partial r}\right) \qquad \text{(A-12)}$$

$$S_{zz} = \frac{2}{1+\lambda_1}f_1(r)\left\{1 + \lambda_2\delta_s\left(v_c\frac{\partial}{\partial r} + \frac{u_c}{\delta_s}\frac{\partial}{\partial z}\right)\right\}\left(\frac{\partial u_c}{\partial\bar{z}}\right) \qquad \text{(A-13)}$$

$$S_{\theta\theta} = \frac{2\epsilon}{1+\lambda_1}f_1(r)\left\{1 + \lambda_2\delta_s\left(v_c\frac{\partial}{\partial r} + \frac{u_c}{\delta_s}\frac{\partial}{\partial z}\right)\right\}\left(\frac{u}{r}\right) \qquad \text{(A-14)}$$

and $f_1(r) = 1 + \beta_1 h_m(R_1^{m_2} - r^{m_2})$. The non-dimensional retardation time may be defined as $\lambda_2 = \frac{\bar{\lambda}_2\bar{u}_0}{\bar{L}_0}$.

In the initial stage of mild stenosis, $\delta_s = \frac{\bar{\delta}_s}{\bar{R}_0} << 1$; in this case, from Eq. (A-8), $\frac{\partial u_c}{\partial z} << 1$. Using the assumptions in [1, 4, 10] subject to the conditions

(i) $\frac{Re\bar{\delta}_s n_1^{\frac{1}{n_1-1}}}{L_0} << 1$ and (ii) $\epsilon n_1^{\frac{1}{n_1-1}} \sim \mathrm{O}(1)\,(\epsilon = \frac{\bar{R}_0}{L_0})$,

the lumen radius is very small compared to the wavelength of pressure wave, equation of motion in radial direction (A-10) will reduce to $\frac{\partial p}{\partial r} = 0$ [53] and low-Reynolds-number approximation [54, 55], and the momentum equations become

$$\frac{\alpha^2}{\rho_0}\frac{\partial u_c}{\partial t} = -\frac{\partial p}{\partial z} + \left(\frac{1}{1+\lambda_1}\right)\frac{1}{r}\frac{\partial}{\partial r}\left[1 + \beta h_m\left(R_1^{m_2} - r^{m_2}\right)\right]\frac{\partial u_c}{\partial r}$$
$$- M^2(r)u_c, \qquad \text{(A-15)}$$

$$\frac{\partial p}{\partial r} = 0. \qquad \text{(A-16)}$$

Similarly, the governing equation for Newtonian fluid in peripheral plasma region can be obtained by performing an order of magnitude analysis as done here. For further details regarding the order of magnitude analysis, see references [56, 57].

References

[1] Young D F 1968 Effects of a time-dependent stenosis on flow through a tube. *Trans. ASME J. Eng. Ind.* 90: 248–254

[2] Young D F and Tsai F Y 1973 Flow characteristic in models of arterial stenosis-I: steady flow. *J. Biomech.* 6: 395–410

[3] Chaturani P and Ponnalagarsamy R 1986 Pulsatile flow of Casson's fluid through stenosed arteries with applications to blood flow. *Biorheology* 23: 499–511

[4] Ponalagusamy R 1986 *Blood flow through stenosed tube*. Ph.D Thesis. Bombay, India: IIT

[5] Young D F 1979 Fluid mechanics of arterial stenosis. *Trans. ASME J. Biomech. Eng.* 101: 157–175

[6] Caro C G 1981 Arterial fluid mechanics and atherogenesis. *Recent Adv. Cardiovas. Dis.* 2(Suppl.): 6–11

[7] Ku D N 1997 Blood flow in arteries. *Annu. Rev. Fluid Mech.* 29: 399

[8] Kumar S and Kumar D 2009 Research note: Oscillatory MHD flow of blood through an artery with mild stenosis. *IJE Trans. A: Bas.* 22: 125–130

[9] Chaturani P and Ponnalagarsamy R 1983 Blood flow through stenosed arteries. In: *Proceedings of the First International Conference on Physiological Fluid Dynamics*, pp. 63–67

[10] Mekheimer K S and EI Kot M A 2008 The micropolar fluid model for blood flow through a tapered artery with a stenosis. *Acta Mech. Sin.* 24: 637–644

[11] Bloch E H 1962 A quantitative study of the hemodynamics in the living microvascular system. *Am. J. Anat.* 110: 125–153

[12] Jeffords J V and Knisley M H 1956 Concerning the geometric shapes of arteries and arteriols. *Angiology* 7: 105–136

[13] El-Shahed M 2003 Pulsatile flow of blood through a stenosed porous medium under periodic body acceleration. *Appl. Math. Comput.* 138: 479–488

[14] El-Shehawey E F, Eibarbary E M E, Afifi N A S and El-Shahed M 2000 Pulsatile flow of blood through a porous medium under periodic body acceleration. *Int. J. Theoret. Phys.* 39: 183–188

[15] Sharma M K, Bansal K and Bansal S 2012 Pulsatile unsteady flow of blood through porous medium in a stenotic artery under the influence of transverse magnetic field. *Korea-Australia Rheol. J.* 24: 181–189

[16] Chaturani P and Ponnalagarsamy R 1984 Analysis of pulsatile blood flow through stenosed arteries and its applications to cardiovascular diseases-I. In: *Proceedings of the 13th National Conference on Fluid Mechanics and Fluid Power*, pp. 463–468

[17] El-Shehawey E F, Eibarbary E M E, Afifi N A S and El-Shahed M 2000 MHD flow of an elastic-viscous fluid under periodic body acceleration. *J. Math. Sci.* 23: 795–799

[18] Ramachandra Rao A and Deshikachar K S 1988 Physiological type flow in a circular pipe in the presence of a transverse magnetic field. *J. Indian Inst. Sci.* 68: 247–260

[19] Haldar K and Ghosh S N 1994 Effect of a magnetic field on blood flow through an indented tube in the presence of erythrocytes. *Indian J. Pure Appl. Math.* 25: 345–352

[20] Voltairas P A, Fotiadis D I and Michalis L K 2002 Hydrodynamics of magnetic drug targeting. *J. Biomech.* 35: 813–821

[21] Vardanian V A 1973 Effect of magnetic field on blood flow. *Biofizika* 18: 491–496

[22] Bhargava R, Rawat S, Takhar H S and Beg O A 2007 Pulsatile magneto-biofluid flow and mass transfer in a non-Darcian porous medium channel. *Meccanica* 42: 247–262

[23] Ponalagusamy R and Tamil Selvi R 2015 Influence of magnetic field and heat transfer on two-phase fluid model for oscillatory blood flow in an arterial stenosis. *Meccanica* 50: 927–943

[24] Mathur P and Jain S 2011 Pulsatile flow of blood through a stenosed tube: effect of periodic body acceleration and a magnetic field. *J. Biorheol.* 25: 71–77

[25] Motta M, Haik Y, Gandhari A and Chen C J 1998 High magnetic field effects on human deoxygenated hemoglobin light absorption. *Bioelectrochem. Bioenerg.* 47: 297–300

[26] Midya C, Layek G C, Gupta A S and Roy Mahapatra T 2003 Magnetohydrodynamic viscous flow separation in a channel with constrictions. *ASME. J. Fluid Eng.* 125: 952–962

[27] Nadeem S and Ijaz S 2015 Theoretical analysis of metallic nanoparticles on blood flow through stenosed artery with permeable walls. *Phys. Lett. A* 379: 542–554

[28] Bugliarello B and Sevilla J 1970 Velocity distribution and other characteristics of steady and pulsatile blood flow in fine glass tubes. *Biorheology* 7: 85–107

[29] Cokelet G R 1972 The rheology of human blood. In: *Biomechanics* N.J.: Prentice-Hall, Englewood Cliffs

[30] Ponalagusamy R 2007 Blood flow through an artery with mild stenosis, a two-layered model, different shapes of stenoses and slip velocity at the wall. *J Appl Sci.* 7: 1071–1077

[31] Chaturani P and Ponnalagarsamy R 1982 A two layered model for blood flow through stenosed arteries. In: *Proceedings of the 11th National Conference on Fluid Mechanics and Fluid Power*, pp. 16–22

[32] Ponalagusamy R and Tamil Selvi R 2011 A study on two-layered model (Casson-Newtonian) for blood flow through an arterial stenosis: axially variable slip velocity at the wall. *J. Franklin Inst.* 348: 2308–2321

[33] Sankar D S and Lee U 2010 Two-fluid Casson model for pulsatile blood flow through stenosed arteries: a theoretical model. *Commun. Nonlin. Sci. Numer. Simul.* 15: 2086–2097

[34] Srivastava V P 1996 Two phase model of blood flow through stenosed tubes in the presence of a peripheral layer: applications. *J Biomech.* 29: 1377–1382

[35] Chaturani P and Ponnalagarsamy R 1986 Dilatancy effects of blood on flow through arterial stenosis. In: *Proceedings of the 28th Congress of ISTAM*, India, pp. 87–96

[36] Ikbal M A, Chakravarty S, Wong K K L, Mazumdar J and Mandal P K 2009 Unsteady response of non-Newtonian blood flow through a stenosed artery in magnetic field. *J. Comput. Appl. Math.* 23: 243–259

[37] Mustapha N, Amin N, Chakravarty S and Mandal P K 2009 Unsteady magnetohydrodynamic blood flow through irregular multi-stenosed arteries. *Comput. Biol. Med.* 39: 896–906

[38] Eldesoky I M, Kamel M H, Hussien R M and Abumanndour R M 2013 Numerical study of unsteady MHD pulsatile flow through porous medium in an artery using generalized differential quadrature method (GDQM). *Int. J. Mater. Mech. Manuf.* 1(2): 200–206

[39] Akbar N S, Nadeem S, Hayat T and Hendi A A 2012 Effects of heat and chemical reaction on Jeffrey fluid model with stenosis. *Appl. Anal.* 91(9): 1631–1647

[40] Nallapu S and Radhakrishnamacharya G 2014 Jeffrey fluid flow through porous medium in the presence of magnetic field in narrow tubes. *Int. J. Eng. Math.* 2014: 713–831

[41] Jyothi K L, Devaki P and Sreenadh S 2013 Pulsatile flow of a Jeffrey fluid in a circular tube having internal porous lining. *Int. J. Math. Arch.* 4: 75–82

[42] Akbar N S, Nadeem S and Lee C 2013 Characteristics of Jeffrey fluid model for peristaltic flow of chime. *Results Phys.* 3: 152–160

[43] Srinivasa Rao K and Koteswara Rao P 2012 Effect of heat transfer on MHD oscillatory flow of Jeffrey fluid through a porous medium in a tube. *Int. J. Math. Arch.* 3(11): 4692–4699

[44] Akbar N S and Nadeem S 2012 Simulation of variable viscosity and Jeffrey fluid model for blood flow through a tapered artery with a stenosis. *Commun. Theor. Phys.* 57(1): 133–140

[45] Ellahi R, Rahman S U and Nadeem S 2014 Blood flow of Jeffrey fluid in a catheterized tapered artery with the suspension of nanoparticles. *Phys. Lett. A* 378: 2973–2980

[46] Ponnalagarsamy R and Kawahara M 1989 A finite element analysis of laminar unsteady flows of viscoelastic fluids through channels with non-uniform cross-sections. *Int. J. Numer. Methods Fluids* 9: 1487–1501

[47] Haynes R H 1960 Physical basis of the dependence of blood viscosity on tube radius. *Am. J. Physiol.* 198: 1193–1200

[48] Ponnalagusamy R 2012 Mathematical analysis on effect of non-Newtonian behaviour of blood on optimal geometry of microvascular bifurcation system. *J. Franklin Inst.* 349: 2861–2874

[49] Nichols W W and O'Rourke M F 1990 *McDonald's blood flow in arteries.* Sevenoaks, Kent: Edward Arnold

[50] Fung Y C 1984 *Biodynamics: circulation*. New York: Springer-Verlag

[51] Ponalagusamy R and Gopalan N P 1993 Numerical study on steady state, three dimensional atmospheric diffusion of sulphur dioxide and sulphate dispersion with non-linear kinetics. *Int. J. Comput. Fluid Dyn.* 1: 339–349

[52] Gopalan N P and Ponnalagarsamy R 1992 Investigation on laminar flow of a suspension in corrugated straight tubes. *Int. J. Eng. Sci.* 30: 631–644

[53] Shaw S, Murthy P V S N and Pradhan S C 2010 The effect of body acceleration on two dimensional flow of Casson fluid through an artery with asymmetric stenosis. *Open Transport Phenom. J.* 2: 55–68

[54] Bhatti M M and Ali Abbas M 2016 Simultaneous effects of slip and MHD on peristaltic blood flow of Jeffrey fluid model through a porous medium. *Alexandria Eng. J.* 55: 1017–1023

[55] Pontrelli G 1998 Pulsatile blood flow in a pipe. *Comput. Fluids* 27(3): 367–380

[56] Hayat T, Ali N, Asghar S and Siddiqui A M 2006 Exact peristaltic flow in tubes with an endoscope. *Appl. Math. Comput.* 182: 359–368

[57] Vajravelu K, Sreenadh S and Lakshminarayana 2011 The influence of heat transfer on peristaltic transport of a Jeffrey fluid in a vertical porous stratum. *Commun. Nonlin. Sci. Numer. Simul.* 16: 3107–3125